ENHANCEMENT OF A MICROWAVE RADIOMETRY IMAGING SYSTEM'S PERFORMANCE USING LEFT HANDED MATERIALS

M. I. Giamalaki[*] and I. S. Karanasiou

Microwave and Fiber Optics Laboratory, Department of Electrical and Computer Engineering, National Technical University of Athens, Greece

Abstract—Aiming at the enhancement of a non invasive Microwave Radiometry Imaging System's (MiRaIS) attributes, Left Handed Materials (LHM) with negative permittivity and negative permeability simultaneously, have been utilized. The optimization of the system focusing properties is being theoretically explored, implementing a semi-analytical Green's function technique and different matching structures. In the framework of this analysis the head is modeled by a double layered cylinder while a dielectric cylindrical layer consisting of LHM is placed on the surface of the human head model with a view to achieve focusing improvement inside the brain. Numerical code executions have been conducted for two different operating frequencies (0.5 GHz and 1.0 GHz) and for matching layers of various values of thicknesses and electromagnetic properties. The numerical results for the electric field distribution inside the head model, presented in this paper, verify that the LHM can provide an increased sensitivity of the system focusing properties and thus improve its overall performance.

1. INTRODUCTION

A non-invasive and totally passive imaging technique, based on the operation principle of microwave radiometry at low microwave frequencies, has been introduced by the Microwave and Fiber Optics Lab of the National Technical University of Athens. A Microwave Radiometry Imaging System (MiRaIS) has been developed and it mainly consists of an ellipsoidal conductive cavity which ensures the focusing on the brain areas of interest and a multifrequency

---

* Corresponding author: Melpomeni I. Giamalaki (melina@esd.ece.ntua.gr).

sensitive radiometric receiver [1–5] (Fig. 1). Various experimental data
provide promising results concerning the system's ability of detecting
temperature and/or conductivity variation distributions in phantoms
and biological tissues [3–5].

The functionality of the system is based on the geometrical
properties of the ellipsoidal as the chaotic radiation emitted by any
material object, being at a temperature above the absolute zero and
placed at one focal point of the ellipsoidal, is detected by the receiving
antenna, placed at the other focus where convergence is achieved.

The focusing ability of the system in specific cortical areas with
the desired spatial resolution and detection depth is the main desired
feature of the proposed imaging technique. Towards the enhancement
of the system's focusing properties, in previous recent work carried out
by our group, various setups have been investigated aiming to improve
the transition of the diffraction index from air to the head and vice
versa. Specifically, initially the receiving antenna was covered by two
layers of different dielectric properties, then a thin lossless dielectric
layer was placed on the surface of the human head model [1] and various
configurations using lossless dielectric materials placed around the head
models/phantoms or used as filling material inside the ellipsoidal cavity
were also implemented [4, 5]. With appropriate adaptation of values
of the dielectric properties and the thicknesses of each layer, a stepped
change of the refraction index on the scattering objects-air interface has
been achieved, hence a better radiation focusing inside the brain has
been observed. On this basis, a means for further improvement of the
focusing properties of the ellipsoidal reflector is herein investigated.
The main differentiating factor of our new approach is that a thin
matching layer consisting of left handed material (metamaterial) [6–
17] has been placed on the surface of the human head model in order
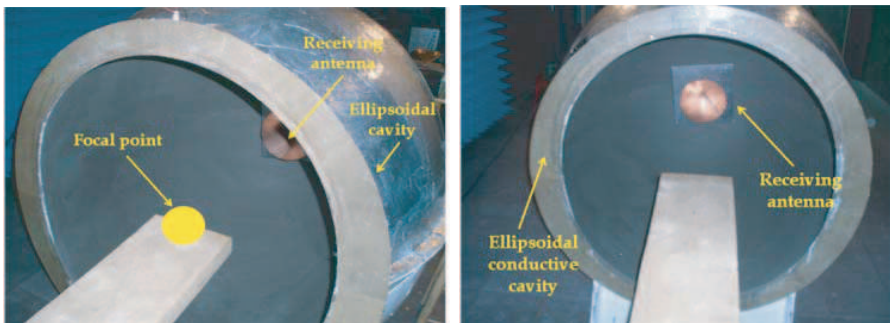to improve the system's performance.

Figure 1. The existing microwave imaging system.

For the purposes of the present research, the scope of modeling the field distribution inside an ellipsoidal conductive cavity in the presence of a human head and especially the focusing properties of the elliptical reflector, is pursued through the implementation of a semi-analytical technique, which is based on the use of the Green's function theory. With a view to assess the focusing optimization of the system in terms of spatial accuracy and penetration depth, a significant number of code executions have been conducted for various matching layers of different thicknesses and electromagnetic properties and the derived numerical results for the electric field distribution inside the head model are presented.

2. THEORETICAL ELECTROMAGNETIC ANALYSIS

The electromagnetic analysis is presented for the case when the human head model is covered by a matching layer consisting of Left Handed Materials in order to improve the transition of the diffraction index at the interface between air and human head. The head is modeled by a double-layered cylinder with radii b_1, and b_2. These two layers are used to simulate different biological media; bone and brain (gray matter) tissues. The head model is surrounded by a cylinder with radii b_3 which is used in order to simulate the LHM layer. The center of the head is placed close to one of the ellipse's focal point on a selected point (x_b, y_b).

The system is excited by two parallel linear current sources of infinite length and opposite sign placed on a selected point (x_a, y_a) close to the second focal point of the ellipsoidal reflector having a distance D from the center of the human head model. The above sources are used to model the dipole antenna and their axes are considered parallel to z-axis. The geometry of the problem is depicted in Fig. 2. It must be noted that a Cartesian coordinate system is used with origin the point of section of the major and minor axes of the ellipse.

The ellipse is defined by the following equation:

$$\frac{x^2}{a^2} + \frac{y^2}{b^2} = 1 \tag{1}$$

The interior of the ellipse is filled with air having wavenumber $k_0 = \omega\sqrt{\varepsilon_0\mu_0}$, where ω is the radian frequency, ε_0 and μ_0 are the free-space permittivity and permeability, respectively. In order to solve this problem, a Green's function technique is adopted [1, 16, 17]. According to the Reciprocity theorem, a response of a system to a source is unchanged when source and measurer are interchanged. Hence, instead
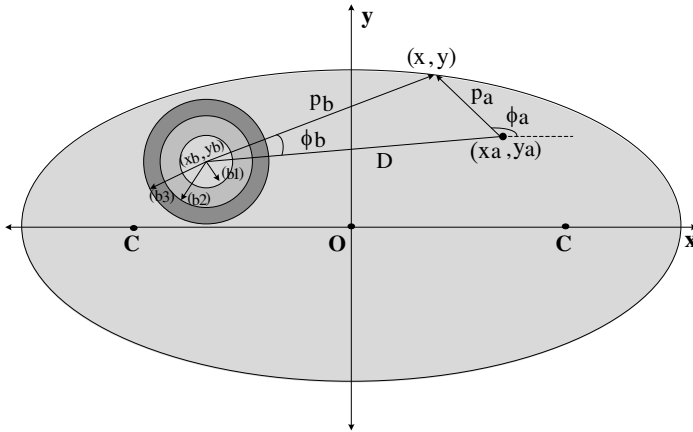
Figure 2. The triple-layered model of the human head and the matching layer placed on a selected point (x_b, y_b), the sources placed on a selected point (x_a, y_a) and the central coordinate system.

of placing the source in the head model, the response of the head model, placed on one focal point of the ellipsoidal cavity, to the excitation generated by the antenna, positioned on the other focus, is calculated.

Initially, the system is examined using a new coordinate system which has origin the center of the triple-layered cylinder that represents the head model covered by a LHM matching layer. By virtue of the cylindrical symmetry of the problem, cylindrical coordinates are used, with unit vectors $\widehat{p}_b$, $\widehat{\phi}_b$. The sources are located in two selected points with cylindrical coordinates p_1 and φ_1 and p_2 and φ_2. The following expressions describe the electric-type Green's functions in the four regions of space. Region 1 demonstrates the area inside the internal cylinder, Region 2 the area inside the middle cylinder, Region 3 the area inside the external cylinder which represents the LHM matching layer and finally Region 4 demonstrates the area between the cylindrical model and the ellipsoidal.

$$\text{Region 1:} \ \Psi_1\left(\vec{p}_b\right) = \sum_{k=-\infty}^{\infty} q_k J_k\left(k_0 n_{b1} \vec{p}_b\right) e^{jk\phi_b} \tag{2}$$

$$\text{Region 2:} \ \Psi_2\left(\vec{p}_b\right) = \sum_{k=-\infty}^{\infty} [S_k J_k(k_0 n_{b2} p_b) + W_k Y_k(k_0 n_{b2} p_b)] e^{jk\phi_b} \tag{3}$$

$$\text{Region 3:} \ \Psi_3\left(\vec{p}_b\right) = \sum_{k=-\infty}^{\infty} [U_k J_k(k_0 n_{b3} p_b) + V_k Y_k(k_0 n_{b3} p_b)] e^{jk\phi_b} \tag{4}$$

$$\text{Region 4: } \Psi_4\left(\vec{p_b}\right) = \sum_{k=-\infty}^{\infty} \left[r_k J_k(k_0 p_b) + t_k Y_k(k_0 p_b)\right] e^{jk\phi b}$$

$$+\Psi_{01}\left(\vec{p_b}, \vec{p_1}\right) + \Psi_{02}\left(\vec{p_b}, \vec{p_2}\right) \tag{5}$$

where $\Psi_{01}(\vec{p_b}, \vec{p_1})$ and $\Psi_{02}(\vec{p_b}, \vec{p_2})$, the contributions of the two sources are given by the following expression:

$$\Psi_{01}(\vec{p_b}, \vec{p_1}) = -\frac{j}{4} \sum_{k=-\infty}^{\infty} J_k(k_0 p_<) H_k^{(2)}(k_0 p_>) e^{jk(\varphi_b - \varphi_1)} \tag{6}$$

$$\Psi_{02}(\vec{p_b}, \vec{p_2}) = -e^{j\delta} \frac{j}{4} \sum_{k=-\infty}^{\infty} J_k(k_0 p_<) H_k^{(2)}(k_0 p_>) e^{jk(\varphi_b - \varphi_1)} \tag{7}$$

where $p_< = \min(p_b, D)$ and $p_> = \max(p_b, D)$ and q_k, S_k, W_k, U_k, V_k, r_k, t_k are unknown coefficients to be determined, $n_{bi} = \sqrt{\varepsilon_i}$, $J_k(k_0 n_{bi}\vec{p_b})$ is the Bessel function of first kind, $Y_k(k_0 n_{bi}\vec{p_b})$ is the Bessel function of second kind and $H_k^{(2)}(k_0 n_{bi}\vec{p_b})$ is the Bessel function of third kind (Hankel function).

The aforementioned unknown coefficients q_k, S_k, W_k, U_k, V_k, r_k, t_k can be determined by the boundary conditions on the interfaces $p_b = b_1$, b_2, b_3. Specifically, in order to satisfy the continuity of the electric and magnetic field, the boundary conditions on the interfaces $p_b = b_1$, b_2, b_3 are imposed by implementing the following expressions:

$$G_i\left(\vec{p}\right) = G_{i+1}\left(\vec{p}\right), \qquad \vec{p} = a_i, \quad i = 1, 2 \tag{8}$$

$$\frac{\partial}{\partial p}\left(G_i\left(\vec{p}\right)\right) = \frac{\partial}{\partial p}\left(G_{i+1}\left(\vec{p}\right)\right), \quad \vec{p} = a_i, \quad i = 1, 2 \tag{9}$$

At this point it must be taken into account that when the external layer consists of left handed material, the expressions derived by Equation (9) for the satisfaction of the continuity of the magnetic field, must change on the interfaces $p_b = b_2$, b_3. Hence:

$$\frac{1}{\mu_0}\frac{\partial \Psi_2}{\partial \rho} = \frac{1}{\mu_3}\frac{\partial \Psi_3}{\partial \rho} \tag{10}$$

$$\frac{1}{\mu_3}\frac{\partial \Psi_3}{\partial \rho} = \frac{1}{\mu_0}\frac{\partial \Psi_4}{\partial \rho} \tag{11}$$

By implementing the orthogonality properties of the cylindrical functions, six linear equations are obtained for the seven unknown coefficients stated above. The remaining boundary condition to be imposed is on the surface of the conductive ellipse, where the electric field must be zero. Hence, a Cartesian coordinate system is used, with origin the point of section of the major and minor axes of the ellipse as shown in Fig. 2.

As stated above, the electric field on the ellipse must be zero, so the following equation can be obtained:

$$\Psi_4(n_i) = \sum_{k=-\infty}^{+\infty} r_k [J_k(k_0 p_b) + z_k Y_k(k_0 p_b)] e^{jk\phi_b}$$

$$+ \sum_{k=-\infty}^{+\infty} P_k Y_k(k_0 p_b) e^{jk\phi_b} + \Psi_3(p_a, \phi_a) = 0 \qquad (12)$$

where

$$\Psi_3(p_a, \varphi_a) = -\frac{j}{4} \sum_{k=-\infty}^{\infty} J_k(k_0 p_<) H_k^{(2)}(k_0 p_>) e^{jk(\varphi_a - \varphi_1)}$$

$$-e^{jk}\frac{j}{4} \sum_{k=-\infty}^{\infty} J_k(k_0 p_<) H_k^{(2)}(k_0 p_>) e^{jk(\varphi_a - \varphi_2)} \qquad (13)$$

where $p_< = \min(p_a, D)$ and $p_> = \max(p_a, D)$. z_k and P_k are known coefficients that contain the six remaining coefficients: q_k, S_k, W_k, U_k, V_k, t_k and r_k is the only unknown coefficient.

The estimation of the electric field, is obtained from the Equation (12) by assessing the only unknown coefficient r_k. The infinite sum with respect to k is convergent and, hence, it can be truncated to a finite one. Therefore, Equation (12) is applied on a mesh of $(2N+1)$ collocation points on the surface of the ellipsoidal. The position of each collocation point is determined by the following expressions for p_a, φ_a, p_b, φ_b referring to the central coordinate system:

$$p_a = \sqrt{(a\cos n_i - x_a)^2 + (b\sin n_i - y_a)^2} \qquad (14)$$

$$p_b = \sqrt{(a\cos n_i - x_b)^2 + (b\sin n_i - y_b)^2} \qquad (15)$$

$$\phi_a = \tan^{-1}\frac{(b\sin n_i - y_a)}{(a\cos n_i - x_a)} \qquad (16)$$

$$\phi_b = \tan^{-1}\frac{(b\sin n_i - y_b)}{(a\cos n_i - x_b)} \qquad (17)$$

where

$$n_i = \frac{2\pi}{2N+1}i, \quad i = 0, \dots 2N \qquad (18)$$

It is evident that the electric field can be calculated at any point inside the ellipse as well as inside the human head model, with low computational cost.

Various scenarios may be theoretically investigated for different setups and the electric field distribution may be derived from the above analysis by imposing the appropriate values for the dielectric properties and dimensions of the matching LHM used.

3. NUMERICAL RESULTS

Based on the above theoretical analysis, the calculation of the electromagnetic field in the interior of a human head model is carried out, when it is placed in the area of the one focal point of the ellipsoidal cavity and the system is excited by a source placed in the other focal point. Our present research focuses on the consequences of placing different matching layers consisting of left handed material on the surface of the human head model, to the focusing properties and thus the performance of the proposed Imaging System.

The dimensions of the ellipse used for the computation were the actual dimensions of the ellipsoidal reflector that has been constructed in our laboratory: $a = 75\,\text{cm}$ and $b = 60\,\text{cm}$ with inter focal distance $2c = 2\sqrt{a^2 - b^2} = 90\,\text{cm}$. The problem was solved for the frequency $f_1 = 0.5\,\text{GHz}$. The head model, including skull and thick brain (gray matter) is of total diameter 16 cm with $b_1 = 7\,\text{cm}$ and $b_2 = 8\,\text{cm}$ and the dielectric properties of the tissue composition used for the computation for the particular frequency are $\varepsilon_1 = 48.417667$, $\sigma_1 = 0.626460$ for the brain (grey matter) and $\varepsilon_2 = 17.447731$, $\sigma_2 = 0.177212$ for the skull [18]. The magnetic properties of the head model's layers are denoted as $\mu_1 = \mu_2 = \mu_0$.

3.1. Evaluation of the Optimization of the Focusing Properties Using a Matching Layer Consisting of Left Handed Materials

The main issue that is being examined is whether the addition of a matching layer consisting of left handed material on the surface of the human head leads to focusing improvement. The estimation of the electric field distribution inside the head model can be achieved through a numerical code that has been established for the solution of the above described theoretical problem, by implementing the proper changes and setting specific values for each different scenario.

The simulated configurations are as follows: Case 1: The centre of the double layered cylindrical head model is placed at the ellipsoidal focal point while the receiving antenna is placed at the other focal point. Then a similar setup is examined but with the head model surrounded by a layer of left handed material. Case 2: Following the

system focusing properties were tested when an arbitrary area of the
head model is placed at the ellipsoidal focal point (the center of the
head model is moved vertically by 6 cm away of the focal point) with
and without the addition of the surrounding metamaterial matching
layer.

The values used for the numerical code execution are 1 cm of
and diffraction index $n = -1$ for the matching layer. The number
of terms required for the infinite sums to converge and hence to ensure
convergence of the obtained solution at any point is $N = 14$ at 0.5 GHz.
The continuity of the fields at the $r = a_1$, a_2, b_1, b_2 and b_3 between
different layers as well as the boundary conditions on the ellipse have
been checked and verified numerically. The computation results are
depicted in Fig. 3.

The above images indicate that the addition of a matching layer
consisting of left handed materials results in an evident improvement
of the focusing properties. Specifically, when the center of the head
is moved away from the system's geometrical focal area, the field
convergence is distinguishable at the specific region area that is actually
placed at the ellipsoidal focal point and in this way a focusing area
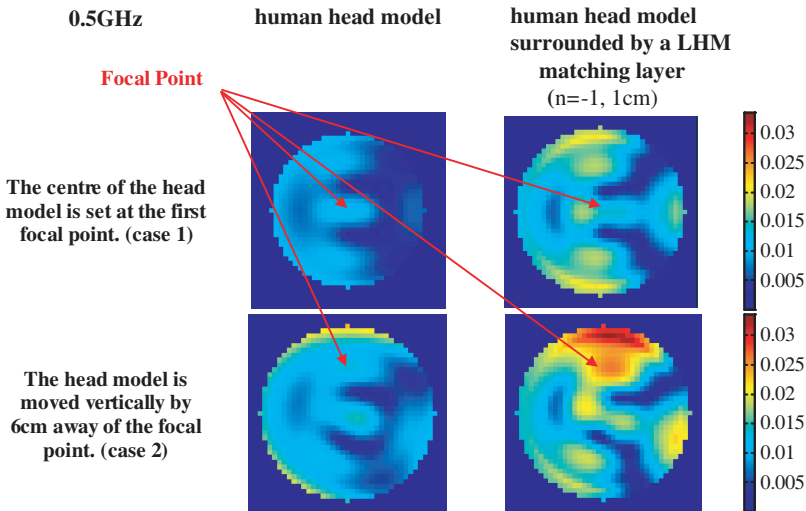inside the human head model is established.

Figure 3. The field distribution inside a double-layered human head
model and the field distribution when it is covered by a matching layer
consisting of metamaterial, for two different cases, at 0.5 GHz.

3.2. The Head Model Surrounded by Layers of Left Handed Materials of Various Properties

Following the focusing achieved inside the human head model, in relation to the electromagnetic properties and the thickness of the matching layer is being examined.

The addition of matching layers consisting of left handed material of various values of thickness and dielectric properties was theoretically examined. Particularly, the input data for the numerical code executions, concerning the properties of the surrounding layer, were $n = -1$ for the first case, $n = -2$ for the second case and $n = -3$ for the third case while their thickness varies from $1\,\text{cm}$ to $2\,\text{cm}$. In all of the above mentioned cases an arbitrary area of the head model is placed at the ellipsoidal focal point.

The number of terms required for the infinite sums to converge is $N = 14$ at $0.5\,\text{GHz}$. The continuity of the fields at the $r = b_1$, b_2 and b_3 between different layers has been checked and verified numerically as well as the validity of the boundary conditions on the ellipse.

The results depicted in Fig. 4 are showing the electric field distribution inside the head model when it is surrounded by layers consisting of metamaterials of three different diffraction indices and two different thickness values, $1\,\text{cm}$ and $2\,\text{cm}$ respectively and its center is moved vertically by $6\,\text{cm}$ away of the focal point at the frequency of $0.5\,\text{GHz}$.

By observing the above figures the contribution of matching layers consisting of left handed materials to the system's focusing properties optimization can be verified. The focusing areas formed at the head model area that is placed at the focal point of the ellipsoidal are distinguishable for all the combinations of properties of the matching layer that surrounds the head model. However, the biggest convergence of the field in the focusing area is observed when the layer consists of the material with $n = -2$ of $1\,\text{cm}$ thickness. In addition, it can be derived that while using the material $n = -1$ of $1\,\text{cm}$ thickness, a more strict determination of the area placed at the focal point is achieved since a smaller surface of intense focusing is appeared and the bounds of the focusing area are better delimited and defined. Regarding the thickness of the matching layer, it is concluded that the $1\,\text{cm}$ thick layer of metamaterial in all cases is considered adequate for the optimization of the penetration depth and the focusing properties of the proposed system.
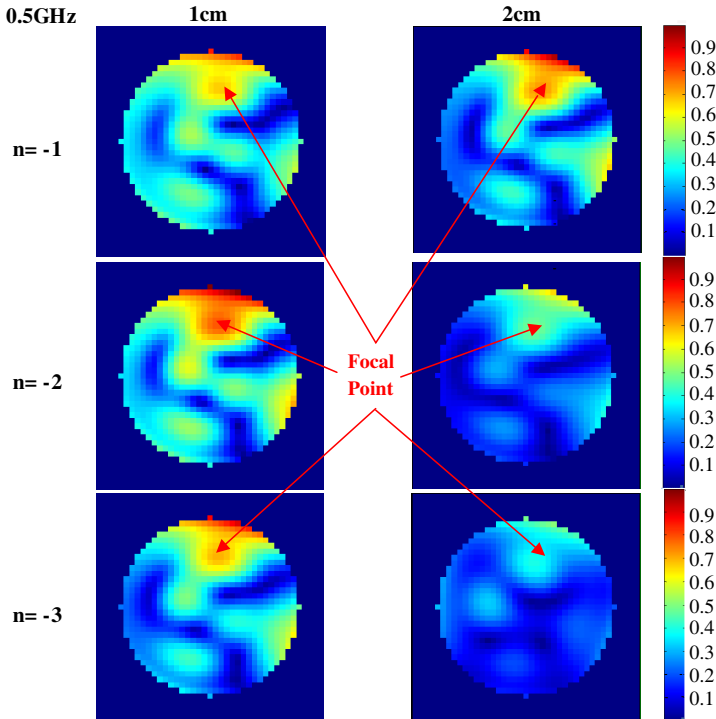
Figure 4. The field distribution depicted only inside the head model, when it is surounded by various matching layers consisting of metamaterial, at 0.5 GHz. The head model is moved vertically by 6 cm away of the focal point.

4. DISCUSSION AND CONCLUSIONS

The possibility of the enhancement of the MiRaIS's performance using a matching structure consisting of left handed materials was theoretically investigated in the present paper. A theoretical electromagnetic analysis was performed and the results clearly demonstrated that with negative permittivity and negative permeability simultaneously, the LHM provide the desirable improvement of the system's detection depth and focusing properties.

Specifically, various numerical code executions were performed when the head was simulated by a double layered cylinder and when the same head model was surrounded by a third layer consisting of left handed materials. Through the comparison of the resulting field distributions, it was concluded that when the head was covered

by a matching layer, an increased spatial sensitivity of the system focusing properties was observed when the head was moved away from the system's geometrical focal area while the penetration depth was significantly improved.

Following, more simulation scenarios were investigated using matching LHM layers of different dielectric properties and thicknesses, placed on the surface of the head model. It must be emphasized that the focusing areas generated in the relevant points of the head that were placed at the focal point, were clearly distinguished for all the examined combinations of metamaterials of different dielectric properties and different thicknesses, at the particular frequency. The exact area of the head model that was located in the focal point of the ellipsoidal cavity could be identified by the small region surfaces where the focusing was intense. By comparing, the resulted images of the different scenarios regarding the penetration depth and the system's focusing properties, it is concluded that the most improved system focusing attributes were achieved when the matching layer was consisted by LHM with diffraction index $n = -2$ and its thickness was 1 cm. Finally, it is concluded that for all the different dielectric properties of the materials that have been examined, the thickness of 1 cm was considered adequate for the optimization of the penetration depth and the focusing properties of the proposed system.

By inference, the use of matching structures consisting of left handed materials, placed on the surface of a human head model, provides an upgraded imaging system, with significantly enhanced focusing attributes, optimized sensitivity and larger penetration/detection depth and thus improved performance.

REFERENCES

1. Giamalaki, M. I., I. S. Karanasiou, and N. K. Uzunoglu, "Electromagnetic analysis of a non invasive microwave radiometry imaging system emphasizing on the focusing sensitivity optimization," *Progress In Electromagnetic Research*, Vol. 90, 385–407, 2009.
2. Karanasiou, I. S., N. K. Uzunoglu, and A. Garetsos, "Electromagnetic analysis of a non-invasive 3D passive microwave imaging system," *Progress In Electromagnetics Research*, Vol. 44, 287–308, 2004.
3. Karanasiou, I. S., N. K. Uzunoglu, and C. Papageorgiou, "Towards functional noninvasive imaging of excitable tissues inside the human body using focused microwave radiometry," *IEEE Transactions on Microwave Theory and Techniques*, Vol. 52, No. 8, 1898–1908, Aug. 2004.

4. Gouzouasis, I. A., K. T. Karathanasis, I. S. Karanasiou, and N. K. Uzunoglu, "Contactless passive diagnosis for brain intracranial applications: A study using dielectric matching materials," *Bioelectromagnetics*, Vol. 31, No. 5, 335–49, Jul. 2010.

5. Karathanasis, K. T., I. A. Gouzouazis, I. S. Karanasiou, M. I. Giamalaki, G. Stratakos, and N. K. Uzunoglu, "Noninvasive focused monitoring and irradiation of head tissue phantoms at microwave frequencies," *IEEE Transactions on Information Technology in BioMedicine*, Vol. 14, No. 3, 657–663, 2010.

6. Veselago, V. G., "The electrodynamics of substances with simultaneously negative values of ε and μ," *Soviet Physics USPEK*, Vol. 10, 509–514, 1968.

7. Valagiannopoulos, C. A., "Electromagnetic scattering from two eccentric metamaterial cylinders with frequency-dependent permittivities differing slightly each other," *Progress In Electromagnetics Research B*, Vol. 3, 23–34, 2008.

8. Wang, J. F., S. B. Qu, H. Ma, Y. M. Yang, X. Wu, and M. J. Hao, "Wide-angle polarization-independent planar left-handed metamaterials based on dielectric resonators," *Progress In Electromagnetics Research B*, Vol. 12, 243–258, 2009.

9. Antonini, G., "A general framework for the analysis of metamaterial transmission lines," *Progress In Electromagnetics Research B*, Vol. 20, 353–373, 2010.

10. Yu, G. X., T. J. Cui, W. X. Jiang, X. M. Yang, Q. Cheng, and Y. Hao, "Transformation of different kinds of electromagnetic waves using metamaterials," *Journal of Electromagnetic Waves and Applications*, Vol. 23, No. 5–6, 583–592, 2009.

11. Wang, R., J. Zhou, C. Sun, L. Kang, Q. Zhao, and J. Sun, "Left-handed materials based on crystal lattice vibration," *Progress In Electromagnetics Research Letters*, Vol. 10, 145–155, 2009.

12. Wang, J., S. Qu, J. Zhang, H. Ma, Y. Yang, C. Gu, X. Wu, and Z. Xu, "A tunable left-handed metamaterial based on modified broadside-coupled split-ring resonators," *Progress In Electromagnetics Research Letters*, Vol. 6, 35–45, 2009.

13. Gennarelli, G. and G. Riccio, "Diffraction by a lossy double-negative metamaterial layer: a uniform asymptotic solution," *Progress In Electromagnetics Research Letters*, Vol. 13, 173–180, 2010.

14. Zhu, B., C. Huang, Y. Feng, J. Zhao, and T. Jiang, "Dual band switchable metamaterial electromagnetic absorber," *Progress In Electromagnetics Research B*, Vol. 24, 121–129, 2010.

15. Antonini, G., "A general framework for the analysis of metamaterial transmission lines," *Progress In Electromagnetics Research B*, Vol. 20, 353–373, 2010.

16. Essadqui, A., J. Ben-Ali, and D. Bria, "Photonic band structure of 1D periodic composite system with left handed and right handed materials by Green function approach," *Progress In Electromagnetics Research B*, Vol. 23, 229–249, 2010.

17. Jarchi, S., J. Rashed-Mohassel, and R. Faraji-Dana, "Analysis of microstrip dipole antennas on layered metamaterial substrate," *Journal of Electromagnetic Waves and Applications*, Vol. 24, No. 5–6, 755–764, 2010.

18. Gabriel, S., R. W. Lau, and C. Gabriel, "The dielectric properties of biological tissues: II. Measurements in the frequency range 10 Hz to 20 GHz," *Physics in Medicine and Biology*, Vol. 41, 2251–2269, 1996.